Development of high-pressure, high-field and multifrequency electron spin resonance system

Sakurai, Takahiro ; Taketani, Akio ; Tomita, Takahiro ; Okubo, Susumu ; Ohta, Hitoshi ; Uwatoko Yoshiya

(Citation)
Review of Scientific Instruments,78(6):065107-065107

(Issue Date)
2007-06-22

(Resource Type)
journal article

(Version)
Version of Record

(URL)
https://hdl.handle.net/20.500.14094/90000748

Development of high-pressure, high-field and multifrequency electron spin resonance system

T. Sakurai[a)]
Center for Supports to Research and Education Activities, Kobe University, Nada, Kobe 657-8501, Japan

A. Taketani
Graduate School of Science and Technology, Kobe University, Nada, Kobe 657-8501, Japan

T. Tomita, S. Okubo, and H. Ohta
Molecular Photosience Research Center, Kobe University, Nada, Kobe 657-8501, Japan

Y. Uwatoko
Institute for Solid State Physics, University of Tokyo, Kashiwa, Chiba 277-8581, Japan

(Received 6 February 2007; accepted 13 May 2007; published online 22 June 2007)

The electron spin resonance (ESR) system which covers the magnetic field region up to 16 T, the quasicontinuous frequency region from 60 to 700 GHz, the temperature region from 1.8 to 4.2 K, and the hydrostatic pressure region up to 1.1 GPa has been developed. This is the first pulsed high-field and multifrequency ESR system with the pressure region over 1 GPa as far as we know. Transmission ESR spectra under hydrostatic pressure can be obtained by combining a piston-cylinder-type pressure cell and the pulsed magnetic field ESR apparatus. The pressure cell consists of a NiCrAl cylinder and sapphire or zirconia inner parts. The use of sapphire or zirconia as inner parts enables us to observe ESR under pressure because these inner parts have high transmittance for the electromagnetic wave with millimeter and submillimeter wavelengths. We have successfully applied this system for the pressure dependence measurements of an isolated spin system $NiSnCl_6 \cdot 6H_2O$ up to 1.1 GPa. It was found that the single ion anisotropy parameter D of this compound strongly depends on pressure. The parameter D is approximately proportional to the pressure up to 0.75 GPa, and the relation between D and the pressure can be used for the pressure calibration of this high-field and high-pressure ESR system. © *2007 American Institute of Physics.*
[DOI: 10.1063/1.2746818]

I. INTRODUCTION

Pressure is one of the most important parameters as well as temperature and magnetic field in research field of condensed matter physics. It is a direct method to change lattice parameters of solid crystals continuously, and it also induces a great variety of interesting phenomena. Electron spin resonance (ESR) is one of the most reliable methods to detect electron spins and obtain information about magnetic properties of materials from the microscopic point of view. Several types of high-pressure ESR system have been developed so far in the X (~10 GHz), K (~24 GHz), Q (~34 GHz), and V bands (~75 GHz).[1] They display their high abilities to investigate magnetic properties of materials under pressure. The first ESR measurement under pressure was done in 1957 at room temperature up to about 1 GPa by a combination of an X-band ESR apparatus and a bomb type pressure cell which includes a coaxial resonator.[2] A pressure region was already achieved up to 10 GPa in an X-band system using a diamond anvil cell whose gasket acts as a resonator.[3] In order to obtain high resolution of the magnetic field, a V-band high-pressure ESR system equipped with a pressure apparatus having a crystal resonator was developed.[4] In the development of these high-pressure ESR systems, a lot of efforts have been paid for combining a resonator with a pressure apparatus to obtain high sensitivity. A diamond anvil cell with double-stacked dielectric resonators has obtained satisfactorily high sensitivity at the X band recently.[5]

There has been a simple transmission-type ESR system which has high sensitivity by gaining a high Zeeman energy under a pulsed high magnetic field. Most of high-pressure ESR systems use resonators, in which the frequency cannot be changed essentially. On the other hand, the transmission-type ESR system without a resonator has an advantage that a large zero-field gap can be determined directly with high energy resolution because the frequency is swept widely as well as the magnetic field. It has turned out that the pulsed high-field and multifrequency ESR is a useful tool to study magnetic materials, particularly ground states and low-lying excited states of quantum spin systems.[6] As pressure also affects interactions such as a spin exchange interaction and a spin-phonon coupling through the change of lattice parameters, an introduction of pressure as a new parameter to the high-field and multifrequency ESR gives us fruitful information about the quantum spin systems from the microscopic point of view.

We have developed pulsed high-field, multifrequency, and high-pressure ESR systems up to 0.35 GPa (Refs. 7–10)

[a)]Electronic mail: tsakurai@kobe-u.ac.jp

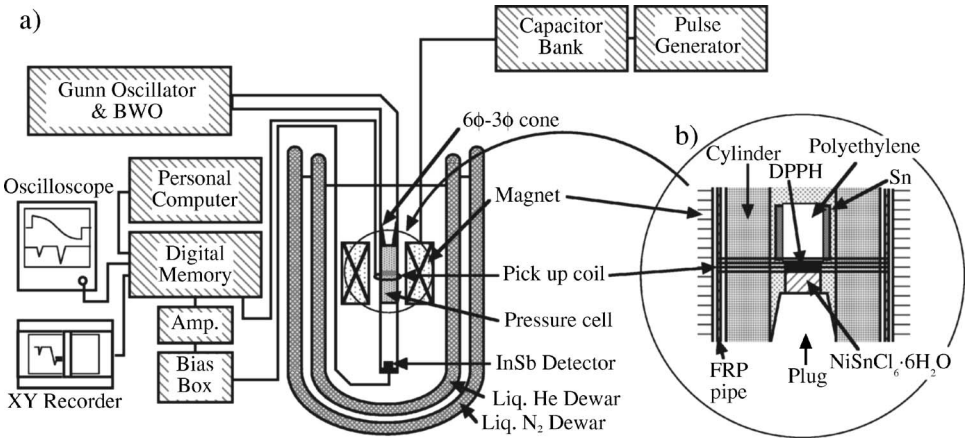

FIG. 1. (a) Schematic diagram of the high-pressure, high-field, and multifrequency ESR system. (b) The side view around a sample in the pressure cell. This figure shows the setting for the pressure dependence measurements of $NiSnCl_6 \cdot 6H_2O$. The Teflon tube is not drawn for simplicity.

and up to 0.6 GPa (Ref. 11) so far. Hydrostatic pressure is generated by a piston-cylinder-type pressure cell, and it is combined with a high-field ESR apparatus which was developed in our laboratory.[6,12] They are the first attempts of the high-pressure ESR measurements using the pulsed magnetic field as far as we know. In this article, we will present a further improved system which reaches a pressure of 1.1 GPa. A few problems caused by an eddy current,[9,10] which often disturb precise measurements in experiments with a combination of the pulsed magnetic field and the pressure cell, have been almost solved in this system. In addition to the outline of this ESR system, an application to an isolated spin system will be demonstrated. As the resonance fields of this compound show large pressure dependence, it can be used as a pressure standard for this ESR system. This result also shows that the high-pressure, high-field, and multifrequency ESR system is a powerful tool to study magnetic materials under pressure.

II. SYSTEM OUTLINE

The developed pulsed high-field, multifrequency, and high-pressure ESR system is schematically shown in Fig. 1(a). A pulsed magnetic field is generated by a combination of a capacitor bank with the maximum stored energy of $E \sim 23$ kJ and a pulse magnet with the inductance of $L \sim 2.6$ mH. The capacitance of the capacitor bank is $C \sim 5$ mF. The pulse magnet is made of 0.5ϕ Cu wire and consists of ten layers with 100 turns per layer. The dimensions of the magnet, including a core and supports, are 27ϕ in outer diameter, 9.4ϕ in inner diameter, and 70 mm in height. A sinusoidally time-dependent pulsed magnetic field with a duration time of $\pi\sqrt{LC} \sim 11$ ms is generated. The maximum magnetic field is restricted up to 16 T, which corresponds to the charging voltage of $V \sim 600$ V, and the pulse magnet can be used repeatedly below 16 T. A clamped-type piston-cylinder pressure cell (Fig. 2), which is widely used in the magnetic susceptibility measurements,[13] is inserted into the magnet. The most characteristic feature of this pressure cell is that all inner parts of the pressure cell are made by zirconia or sapphire. These materials show relatively high transmittance of the electromagnetic wave with a wavelength in millimeters or submillimeters. The electromagnetic wave from the light source passes through a 6ϕ stainless light pipe and a sample space of the pressure cell with an inner diameter of 3 mm. The light pipe and the pressure cell are connected optically by a $6\phi-3\phi$ light cone, as shown in Fig. 1(a). The transmitted electromagnetic wave is detected by the 4.2 K InSb detector. Then, transmission ESR spectra of a sample subjected to a certain pressure can be obtained. We have Gunn oscillators (30–60 GHz), their multipliers (180, 210, 240, 260, 300, and 315 GHz), and the backward traveling wave oscillator (BWO) (150–1200 GHz) as the light sources. Although the inner diameter of the cylinder of the pressure cell corresponds to the cutoff frequency of 100 GHz (3 mm) as a waveguide, the frequency above 60 GHz can be applied experimentally in this transmission-type ESR. On the other hand, we succeeded in observing ESR up to 700 GHz (Ref. 11), and the measurements at higher frequencies seem to be possible if the appropriate detector is used. The position of the pressure cell is adjusted so that a sample in the pressure cell is located at the center of the magnet in height. The magnetic field is detected by an ordinary induction method. As shown in Fig. 1(b), a thin pickup coil, which is wound on a fiber reinforced plastics (FRP) pipe, is inside the

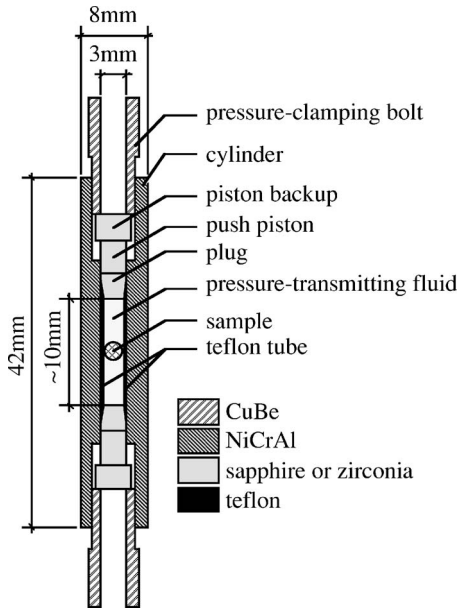

FIG. 2. Cross section of the clamped-type piston-cylinder pressure cell for high-field ESR measurements.

magnet bore and is outside the pressure cell so that it is located just at the center of the magnet in height. Therefore, the pickup coil is on the same height with the sample. At the same time when a pulsed magnetic field is triggered, both an induced voltage at the pickup coil and an ESR signal voltage through an amplifier from the InSb detector are stored as a function of time in a digital memory. And they are sent to a personal computer and are analyzed. The magnetic field inside the pressure cell is calibrated by a field standard which is set in the pressure cell. We use diphenylpicrylhydrazyl (DPPH) with the g value of 2.00 as a field standard. As the inner Dewar vessel is filled with liquid He and the pressure cell is in liquid He, we can make measurements at 4.2 K and at lower temperatures down to 1.8 K, which are obtained by pumping liquid He.

The cross section of the pressure cell is shown in Fig. 2. The cylinder and the clamping bolts of the pressure cell are made by NiCrAl alloy and CuBe alloy, respectively. The inner and outer diameters of the cylinder is 3 and 8 mm, respectively. The pressure at least up to about 1.1 GPa is available at low temperature, as is described below in detail. The height of the sample space in the pressure cell is about 10 mm at maximum before a load is applied. A Teflon tube is used as a pressure seal. It is also expected to suppress a heat flow from the cylinder to the sample space when a Joule heat is generated at the cylinder under the pulsed magnetic field. A mixture of Fluorinert FC70:FC77=1:1 is used as a pressure-transmitting fluid and is also confirmed to have good transmittance in the wide frequency region and no intrinsic ESR signal. It should be noted that this type of pressure cell can be applied to any transmission-type ESR apparatus. In our laboratory, a new capacitor bank with an energy of 300 kJ has been set up recently and an ESR system with a 55 T pulse magnet is now available.[14] We plan to extend the magnetic field region of high-pressure ESR measurements by this 55 T magnet.

III. EDDY CURRENT EFFECT

A pulsed magnetic field induces an eddy current in metal parts of the pressure cell. The eddy current converts into a Joule heat. Consequently, it causes a heating of a sample when a heat flow occurs from the pressure cell to a sample.[9,10] The important physical quantities are the electric resistance of the cylinder and the thermal diffusivities of materials between a sample and the cylinder. Since the electric resistance of the cylinder determines the quantity of the eddy current, the higher resistance cylinder has a lower Joule heat that occurs under the same charging voltage. The resistivities of CuBe and NiCrAl alloys are 6–8 and 60–70 $\mu\Omega$ cm at room temperature, respectively.[15] Therefore, it is expected that the Joule heat due to the eddy current is more suppressed in a NiCrAl cylinder. The thermal diffusivities of materials between a sample and the cylinder govern the temperature distribution in the sample space during the duration time of a pulsed field ($\sim$11 ms). The order of the magnitude of the thermal diffusivity of sapphire is 10^{-1} m^2/s at low temperature, while Teflon and liquid He have relatively low diffusivities ($\sim 10^{-6}$ and $\sim 10^{-8}$ m^2/s, respectively).[16] Organic materials such as Fluorinert are expected to have a similar order of the magnitude of the diffusivity with that of Teflon. Therefore, the Joule heat which occurs in the cylinder may flow into a sample through a sapphire plug within the duration time in the case that a sample is directly set on the sapphire plug, or it may flow into a sample directly in the case that a sample is in contact with a cylinder without a Teflon tube. In a measurement of a quantum spin system $CsCuCl_3$ at 4.2 K with the CuBe cylinder and without a Teflon tube, the heating of the sample by about 2 K was actually observed within the duration time.[9,10] On the other hand, it was confirmed in the case of $CsCuCl_3$ that such a heating hardly occurs when the NiCrAl cylinder and Teflon tube are used and the sample is not directly set on a sapphire plug. It is important to use a high resistive alloy as a cylinder and to insulate a sample thermally from the cylinder as a heat source in order to avoid the heating of a sample. It should be mentioned that the thermal diffusivity of zirconia is lower than that of sapphire by about one order of magnitude. The use of zirconia as inner parts is expected to suppress a heat flow into a sample space.

Another problem due to the eddy current is a shielding of the external magnetic field at the sample position because the eddy current flows so as to avoid the penetration of the magnetic field into the inside of the pressure cell. As the magnetic field B varies sinusoidally with time, the sweep rate dB/dt varies cosinusoidally, which implies that the sweep rate is larger at the lower field side and the shielding effect is larger at the higher sweep rate. Therefore, this shielding effect has to be considered when a large magnetic field is generated and a signal is observed at the lower field side. The shielding of the external magnetic field was actually observed when a CuBe cylinder was used.[9] We found a weak but systematic sweep rate dependence of the resonance field for DPPH in the case of a CuBe cylinder. For instance, the resonance field of DPPH was observed to be shifted to the higher field side from the correct position by about 3% when it was observed at around 25% of the maximum magnetic field (corresponding to the sweep rate $dB/dt \sim 4000$ T/s). On the other hand, the resonance field of DPPH was observed at an almost correct position within the error when it was measured at about 80% of the maximum magnetic field ($dB/dt \sim 700$ T/s). As the external magnetic field is detected by the pickup coil outside of the pressure cell, as shown in Fig. 1(b), it detects a higher field than that at the sample position in the pressure cell. It means that in the former case the external magnetic field is shielded by about 3% at the sample position in the pressure cell. In the latter case the shielding effect is negligible due to the lower sweep rate. For the NiCrAl cylinder, however, no sweep rate dependence was observed within the error. It means that the shielding effect is negligible for the NiCrAl cylinder irrespective of the sweep rates of the magnetic field. These results suggest that the eddy current effect is much smaller in the NiCrAl alloy than in the CuBe alloy, and it can be attributed to the higher resistivity of the NiCrAl alloy.

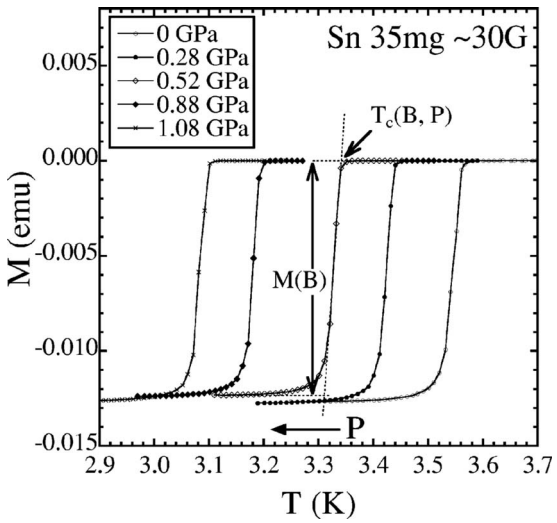

FIG. 3. Typical temperature dependence of the magnetization of tin at various pressures.

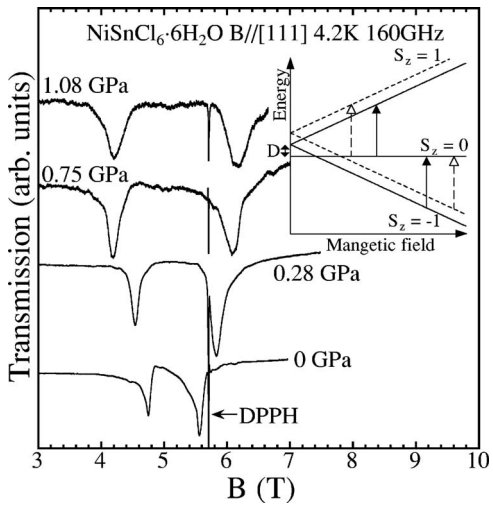

FIG. 4. Pressure dependence ESR spectra of $NiSnCl_6 \cdot 6H_2O$ at 4.2 K obtained at 160 GHz. The inset shows the schematic energy-field diagram of this compound. The arrows indicate the allowed ESR transitions. The solid and broken lines correspond to a case with a smaller D value and a case with a larger D value, respectively.

IV. APPLICATION

In this section we demonstrate an example of the high-field, multifrequency, and high-pressure ESR measurements. The compound is an isolated spin system $NiSnCl_6 \cdot 6H_2O$ whose magnetic ion is Ni^{2+} ($S=1$). The Ni^{2+} ion is in a $[Ni(H_2O)]^{2+}$ octahedron with trigonal distortion. It is known that the anisotropy parameter D in its spin Hamiltonian increases with decreasing temperature.[17] We found that the D value increases with increasing pressure, as described below in detail. In order to measure the pressure dependence of the D value of $NiSnCl_6 \cdot 6H_2O$, we have performed the following experiments: (1) a loading of a pressure, (2) a temperature dependence measurement of magnetization of tin to determine the pressure, and (3) an ESR measurement to determine the D value of $NiSnCl_6 \cdot 6H_2O$. Sequence (1)–(3) was repeated.

$NiSnCl_6 \cdot 6H_2O$ was crystallized by following the procedure in Ref. 18. A single crystal was cleaved along the [111] direction which corresponds to the trigonal axis of a $[Ni(H_2O)]^{2+}$ octahedron. A peace of cleaved crystal was cut perpendicular to the [111] direction with dimensions of $1 \times 1 \times 1$ mm^3. The included number of spins in this sample is $\sim 5 \times 10^{18}$. It should be mentioned that it is not an observable limit of this system. We have observed an ESR signal of ruby, whose number of spins is $\sim 1 \times 10^{16}$, with satisfactorily good sensitivity. The sample was set in the pressure cell with DPPH and tin with 99.999% purity, as shown in Fig. 1(b). The magnetic field was applied parallel to the [111] direction. A weight of the tin used in the experiment was ~35 mg. It was made like a cylinder around a small polyethylene rod, as shown in Fig. 1(b), and was put into the pressure cell so that the cylinder axis is parallel to the propagating direction of the electromagnetic wave in order to avoid reduction of its transmittance. The high field ESR measurements under pressure have been performed at 4.2 K in the frequency region from 80 to 240 GHz at six pressure points.

The pressure was determined by the well-known relation between superconducting transition temperature of tin and pressure.[19] The superconducting transition temperature was observed by the temperature dependence of the magnetization of tin by physical properties measurement system (PPMS) (Quantum Design Co. Ltd.). Figure 3 shows the temperature dependence of the magnetization of tin at various pressures. The maximum pressure in this experiment reached 1.08 GPa. The transition was indicated by a steep drop of the magnetization of tin, and it was observed within a narrow temperature region irrespective of applied pressures, which suggests that the pressure homogeneity is quite good up to 1.08 GPa. The transition temperature $T_c(B,P)$ was defined as an onset of the superconducting transition, as shown in Fig. 3. At one pressure point P, the temperature dependence of the magnetization of tin was measured at each 10 G from about −20 to 40 G. From each measurement at the applied magnetic field B, a transition temperature $T_c(B,P)$ and a magnitude of diamagnetization of tin $M(B)$ were obtained. The transition temperature at the exact zero field $T_c(0,P)$ was determined at each pressure by the extrapolation to zero diamagnetization $M(0)$ in a plot of $T_c(B,P)$ vs $M(B)$ under the assumption that $M(B)$ is proportional to the applied magnetic field B. Then, the pressure was determined by the quadratic expression for pressure[19] within the error of 0.01 GPa.

Next, we will discuss the pressure dependence ESR spectra of $NiSnCl_6 \cdot 6H_2O$. Figure 4 shows the results obtained at 160 GHz. Two absorption lines were observed at each pressure, and the interval of these two lines increased with increasing pressure. We emphasize that clear absorption lines are obtained even at the maximum pressure of 1.08 GPa. The slight lowering of the signal to noise ratio on increasing pressure is due to the lowering of the transmittance of electromagnetic wave by a deformation of tin. The linewidths obtained at 160 GHz also increase from about 0.1 T at 0 GPa to about 0.3 T at 1.08 GPa. As the pressure homogeneity is suggested to be excellent up to the maximum pressure as mentioned above, the increase of the linewidth is not caused by inhomogeneity of pressure. Although an origin

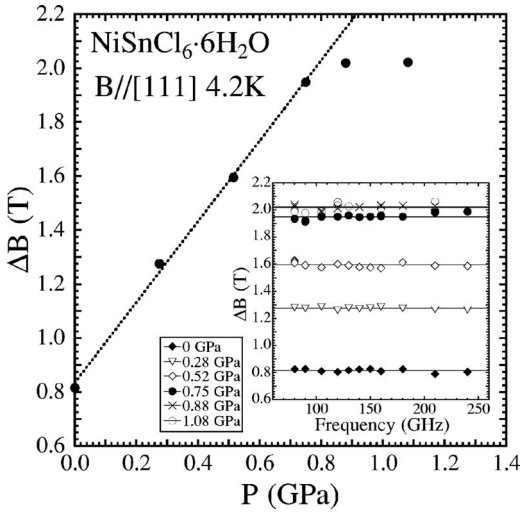

FIG. 5. The pressure dependence of the $\Delta B \equiv B_H - B_L$. The inset is the plot of ΔB vs frequency at various pressures.

of this linewidth behavior is not clear, it seems to be due to the intrinsic nature. From the absorption lines at 0 GPa, we evaluate the sensitivity of this ESR system. The signal to noise ratio for the absorption lines at 0 GPa is about 150. As the number of spins which is included in this sample is the order of the magnitude of 10^{18}, the sensitivity of this system is evaluated to be the order of the magnitude of 10^{17} spins/T (10^{13} spins/G) at 4.2 K. Actually, we have observed ESR signals of a single crystal of ruby by this ESR system with a satisfactorily good signal to noise ratio, whose number of spins and linewidth are about 10^{16} and about 0.01 T, respectively. Figure 5 shows the pressure dependence of the interval of these two resonance fields ΔB. As shown in the inset in Fig. 5, each ΔB point was determined by averaging the intervals obtained in the frequency region from 80 to 240 GHz. The error of the interval was evaluated as the mean error at each pressure. It increases from 0.004 T at 0 GPa to 0.01 T at 1.08 GPa. This error corresponds to 3%–4% of the linewidth at each pressure. As demonstrated in this result, the point that the interval ΔB or the zero-field splitting can be precisely determined within a small error is one of the most important advantages which the high-field and multifrequency ESR system possesses. The error of the interval ΔB is included in the symbol in Fig. 5 as well as the error of pressure. Figure 5 clearly shows that the interval ΔB is very sensitive to pressure, especially below 0.75 GPa. It increases linearly by increasing the pressure and reaches almost 2.5 times of ambient pressure at 0.75 GPa, and it tends to saturate above 0.75 GPa. The origin of this saturating behavior is not clear at present. The dotted line in Fig. 5 is the result of linear fitting to the obtained data up to 0.75 GPa. The relation between the interval of the resonance fields ΔB (T) and pressure P (GPa) of $NiSnCl_6 \cdot 6H_2O$ at 4.2 K is obtained as follows:

$$\Delta B = \alpha P + \beta, \tag{1}$$

where $\alpha = 1.50 \pm 0.05$ T/GPa and $\beta = 0.832 \pm 0.022$ T.

Here, we will discuss the origin of the pressure dependence in ΔB. The spin Hamiltonian of this compound is expressed by

$$\mathbf{H} = g_z \mu_B S_z B_z + D S_z^2 \tag{2}$$

when the magnetic field B is applied parallel to the z-axis which corresponds to the [111] direction, where g_z, μ_B, and D are the g value for the [111] direction, the Bohr magneton, and the single ion anisotropy parameter, respectively. The D value is reported to be positive.[17] As schematically shown in the inset in Fig. 4, the energy-field diagram in the case of $D > 0$ is easily obtained from Eq. (2) bacause the spin quantum numbers are $S_z = 1$, 0, and -1. From the inset, it is apparent that the absorption line at the higher field side and that at the lower field side are due to the transition from $S_z = -1$ to 0 and that from 0 to 1, respectively. These resonance fields are expressed by

$$B_L = \frac{h\nu - D}{g_z \mu_B}, \tag{3}$$

$$B_H = \frac{h\nu + D}{g_z \mu_B}, \tag{4}$$

where B_L and B_H represent the resonance field at the lower field side and that at the higher field side, respectively, and h and ν are the Planck constant and the frequency, respectively. The frequency dependence measurements in the region from 80 to 240 GHz show that the g value was found to be almost unchanged by pressure and it was obtained to be $g_z = 2.21 \pm 0.01$. As the difference of these two absorption lines $\Delta B \equiv B_H - B_L$ is equal to $\Delta B = 2D/g_z \mu_B$ from Eqs. (3) and (4), it is concluded that the increase of the interval of two absorption lines is attributed to the increase of D value by applying the pressure, as shown in the inset in Fig. 4.

As the interval of the resonance fields ΔB strongly depends on the pressure and it increases linearly up to 0.75 GPa, $NiSnCl_6 \cdot 6H_2O$ can be used as a sensitive pressure standard for this ESR system below 0.75 GPa at low temperature. The pressure calibration can be performed with an ESR measurement of a sample at the same time by replacing tin shown in Fig. 1(b) with a sample which is measured. We have already succeeded in the precise pressure dependence measurement of a spin gap system $KCuCl_3$ up to 0.73 GPa by using this calibration method.[20] In the experiment of $KCuCl_3$, a single crystal of $KCuCl_3$ was set in the pressure cell to replace tin, as is mentioned above. Such calibration method is convenient because the pressure calibration and an ESR measurement can be done at the same time. As demonstrated above, the high-pressure, high-field, and multifrequency ESR system is a powerful tool to study magnetic materials under pressure. In addition, a convenient and sensitive pressure calibration method has been established for this ESR system. Therefore, the system is a promising tool to discuss detailed pressure dependence of spin states and to observe a novel pressure-induced phase for magnetic materials from the microscopic point of view.

V. CONCLUSION

The high-field, multifrequency, and high-pressure ESR system has been developed. It consists of the piston-cylinder-type pressure cell and the transmission-type ESR apparatus with a pulse magnet. It is the first pulsed high-field ESR system with the pressure region over 1 GPa. The magnetic field up to 16 T and the temperature region from 1.8 to 4.2 K are available. The hydrostatic pressure can be generated up to about 1.1 GPa. The pressure cell for this ESR system has a characteristic feature that all the inner parts are made of zirconia or sapphire. They enable ESR measurements in the wide frequency region from 60 to 700 GHz because these materials have good transmittance for the electromagnetic wave of this frequency region. Both heating of a sample and shielding of the magnetic field in the pressure cell due to the occurrence of the eddy current in the cylinder are appreciably suppressed under the pulsed magnetic field by using a NiCrAl cylinder. It is attributed to the higher electric resistivity of the NiCrAl cylinder. The heating of a sample is also suppressed by the use of a Teflon tube, which is also used as a pressure seal, because it insulates the Joule heat from the cylinder to a sample thermally. We have confirmed that both problems are almost negligible in the combination of the NiCrAl cylinder and the Teflon tube.

The pressure dependence ESR measurements of an isolated spin system $NiSnCl_6 \cdot 6H_2O$ have been done successfully up to 1.08 GPa at 4.2 K in the frequency region from 80 to 240 GHz. Two absorption lines due to the single ion anisotropy D were observed. The interval of these two absorption lines was found to strongly depend on the pressure. It increases linearly up to 0.75 GPa and it tends to saturate above 0.75 GPa. The pressure dependence of the interval of the resonance fields $\Delta B = 2D/g_z\mu_B$ below 0.75 GPa is obtained to be $\Delta B(\mathrm{T}) = 1.50P(\mathrm{GPa}) + 0.832$ at 4.2 K. It is concluded that the increase of the interval is caused by the increase of the single ion anisotropy D by applying pressure because the g_z is almost not changed by pressure. As the interval ΔB is sensitive to the pressure below 0.75 GPa, it can be used as a pressure standard. It is convenient to use $NiSnCl_6 \cdot 6H_2O$ as a pressure standard because the pressure calibration and an ESR measurement can be done at the same time.

ACKNOWLEDGMENTS

One of the authors (T.S.) would like to thank Dr. T. Takeuchi (Osaka University) and Dr. S. Kimura (Osaka University) for their kind support on the PPMS measurements. This work was supported by a Grant-in-Aid for Scientific Research (No. 17740228) from the Ministry of Education, Culture, Sports, Science, and Technology (MEXT) of Japan. This work was also supported by Grant-in-Aids for Scientific Research on Priority Areas gHigh Field Spin Science in 100T (No. 451) and Novel Functions of Molecular Conductors under Extreme Conditions (No. 427) from MEXT.

[1] For a review, see C. P. Poole, Jr., *Electron Spin Resonance* (Dover, New York, 1996), p. 337.
[2] W. M. Walsh, Jr. and N. Bloembergen, Phys. Rev. **107**, 904 (1957).
[3] N. Sakai and J. H. Pifer, Rev. Sci. Instrum. **56**, 726 (1985).
[4] S. N. Lukin, P. V. Vodolazskii, and S. M. Ryabenko, Sov. J. Low Temp. Phys. **3**, 705 (1977).
[5] S. E. Bromberg and I. Y. Chan, Rev. Sci. Instrum. **63**, 3670 (1992).
[6] H. Ohta, S. Okubo, K. Kawakami, D. Fukuoka, Y. Inagaki, T. Kunimoto, and Z. Hiroi, J. Phys. Soc. Jpn. **72**, 26 (2003).
[7] H. Ohta *et al.*, Physica B **294–295**, 55 (2001).
[8] H. Ohta, T. Sakurai, S. Okubo, M. Saruhashi, T. Kunimoto, Y. Uwatoko, and J. Akimitsu, J. Phys.: Condens. Matter **14**, 10637 (2002).
[9] T. Sakurai *et al.*, J. Phys. Soc. Jpn. **72**, 156 (2003).
[10] T. Sakurai, M. Saruhashi, Y. Inagaki, S. Okubo, H. Ohta, H. Tanaka, and Y. Uwatoko, Physica B **346–347**, 221 (2004).
[11] T. Sakurai, A. Takatani, S. Kimura, M. Yoshida, S. Okubo, H. Ohta, H. Tanaka, and Y. Uwatoko, AIP Conf. Proc. **850**, 1057 (2006).
[12] M. Motokawa, H. Ohta, and N. Makita, Int. J. Infrared Millim. Waves **12**, 149 (1991).
[13] Y. Uwatoko *et al.*, Rev. High Pressure Sci. Technol. **7**, 1508 (1998).
[14] H. Ohta *et al.*, J. Phys.: Conf. Ser. **51**, 611 (2006).
[15] T. Matsumoto, Rev. High Pressure Sci. Technol. **12**, 280 (2002).
[16] The thermal diffusivity is defined by $\alpha \equiv \kappa/c\rho$, where κ, c, and ρ are the thermal conductivity, the specific heat, and the density, respectively. These values are easily found in a general handbook of material properties.
[17] Y. Ajiro, S. A. Friedberg, and N. S. VanderVen, Phys. Rev. B **12**, 39 (1975).
[18] B. E. Myers, L. G. Polgar, and S. A. Friedberg, Phys. Rev. B **6**, 3488 (1972).
[19] T. F. Smith and C. W. Dhu, Phys. Rev. **159**, 353 (1967).
[20] T. Sakurai, A. Taketani, T. Tomita, S. Okubo, H. Ohta, H. Tanaka, and Y. Uwatoko, J. Phys.: Conf. Ser. **51**, 565 (2006).